RESEARCH PAPER

Development and Evaluation of Protease-Loaded Microparticles for Colon-Targeted Delivery in Inflammatory Bowel Disease

Deepak Kashyap*[1], Princy Kashyap[2], Dr. Manoj Kumar[3]

[1]Research Scholar, Department of Pharmacy, Guru Ghasidas Vishwavidyalaya (A Central University) Bilaspur, Chhattisgarh, India

[2]Research Scholar, Department of Pharmacy, Guru Ghasidas Vishwavidyalaya (A Central University) Bilaspur, Chhattisgarh, India

[3]Associate Professor, Department of Pharmacy, Guru Ghasidas Vishwavidyalaya (A Central University) Bilaspur, Chhattisgarh, India

***Corresponding author**

Deepak Kashyap

Research Scholar, Department of Pharmacy, Guru Ghasidas Vishwavidyalaya (A Central University) Bilaspur, Chhattisgarh, India

Email id. - kashyapdeepak198@gmail.com

Abstract:

Inflammatory bowel disease (IBD), including Crohn's disease and ulcerative colitis, is a chronic inflammatory disorder requiring effective and targeted drug delivery. Proteolytic enzymes such as bromelain, papain, and serratiopeptidase possess potential anti-inflammatory and antioxidant properties; however, their therapeutic application is limited by enzymatic degradation and gastric instability. The present study aimed to develop and evaluate protease-loaded microparticles for colon-targeted delivery in IBD management. Microparticles were prepared using the ionic gelation technique and characterized for particle size, zeta potential, entrapment efficiency, morphology, and in vitro drug release. DSC, XRD, and SEM analyses were performed to assess physicochemical properties and surface morphology. The optimized formulation exhibited spherical microparticles with a particle size of 320–450 μm, minimal release under acidic conditions, and sustained release exceeding 85% over 24 hours in simulated colonic medium. The formulation was further investigated for its potential therapeutic efficacy using an experimental animal model of IBD. Overall, colon-targeted protease-loaded microparticles represent a promising approach for protecting proteolytic enzymes during gastrointestinal transit and enhancing localized drug delivery. Further in vivo studies are required to establish their therapeutic efficacy and clinical applicability.

Keywords: Inflammatory bowel disease; Colon-targeted drug delivery; Protease-loaded microparticles; Ionic gelation; Controlled release; Bromelain; Papain; Serratiopeptidase.

How to cite this article: Deepak Kashyap*1 Princy Kashyap2 Dr. Manoj Kumar3. Development and Evaluation of Protease-Loaded Microparticles for Colon-Targeted Delivery in Inflammatory Bowel Disease. Int J Drug Deliv Technol. 2026;16(89s):503-512. DOI: 10.25258/ijddt.16.89s.54.

1. Introduction

Inflammatory bowel disease (IBD), comprising Crohn's disease (CD) and ulcerative colitis (UC), is a chronic inflammatory disorder characterized by recurrent intestinal inflammation, mucosal barrier dysfunction, and dysregulated immune responses. [1] Its pathogenesis involves complex interactions among genetic susceptibility, environmental factors, intestinal dysbiosis, and immune-mediated inflammatory pathways. [2] The sustained release of pro-inflammatory cytokines, including TNF-α, IL-6, IL-12, and IL-23, contributes to epithelial damage and disease progression. The increasing global burden of IBD, together with its associated gastrointestinal symptoms, extraintestinal complications, and reduced quality of life, highlights the need for effective and well-tolerated therapeutic strategies. Conventional IBD treatments include aminosalicylates, corticosteroids, immunomodulators, and biologic agents. [3] Although these therapies can induce and maintain remission, variable treatment responses, adverse effects, and inadequate localization of therapeutic agents remain important challenges. [4] Colon-targeted drug delivery systems offer a potential approach to overcome these limitations by protecting therapeutic compounds during gastrointestinal transit and facilitating localized, controlled release at the site of inflammation. [5] Polymeric microparticles are particularly useful because their composition and physicochemical properties can be tailored to improve encapsulation, gastrointestinal stability, and drug-release behaviour. [6] Intestinal dysbiosis and altered proteolytic activity may further contribute to IBD-associated inflammation through effects on epithelial barrier integrity and inflammatory signalling, including protease-activated receptor pathways. Proteolytic enzymes such as bromelain, papain, and serratiopeptidase have been investigated for their potential anti-inflammatory and other pharmacological activities. [7] However, their application in IBD requires further validation, particularly because enzymatic stability and activity may be compromised under gastrointestinal conditions. Encapsulation within biodegradable polymeric microparticles may help protect these enzymes and support their targeted delivery to the colon. [8] Therefore, the development of colon-targeted protease-loaded microparticles represents a promising formulation strategy for investigating localized enzyme delivery in IBD management. Systematic physicochemical characterization, in vitro release studies under simulated gastrointestinal conditions and subsequent in vivo

evaluation are necessary to establish formulation performance, therapeutic potential, and safety. This approach may contribute to the development of targeted delivery systems designed to improve local therapeutic activity while limiting unnecessary systemic exposure. [9-10]

2. Material and Methods

Preparation of microparticles by ionic gelation method:

Bromelain (100 mg), papain (100 mg), and serratiopeptidase (100 mg) were used as the active proteolytic enzymes. Sodium alginate was procured for matrix formation and employed at concentrations determined by the experimental design (500, 1000, and 1500 mg per batch). [11] Calcium chloride ($CaCl_2$) was utilized to formulate a 3% (w/v) ionic cross-linking solution. Phosphate-buffered saline (PBS, pH 7.0) and deionized/distilled water were used as solvents for enzyme reconstitution and polymer hydration, respectively. All other reagents and chemicals utilized were of analytical grade. [12]

Enteric coating of microparticles

To protect the acid-labile proteolytic enzymes from gastric degradation and facilitate colon-targeted release, the core microparticles were coated with Eudragit® S100, an anionic copolymer insoluble below pH 7.0. The coating level was systematically varied across three levels (5%, 10%, and 15% w/w relative to dry core particle mass) according to the experimental design. [13] The coating solution was formulated by dissolving Eudragit® S100 in a volatile organic solvent mixture of isopropyl alcohol and acetone (1:1 v/v). Polyethylene glycol 400 (PEG 400, 10% w/w based on dry polymer weight) was incorporated as a plasticizer to enhance film flexibility and prevent surface fissuring. [14] The total solid content (W_{solids}) required per batch was determined using Equation (1):

$$W_{solids} = W_{core} \times \left(\frac{L}{100}\right) \times (1 + P)$$

Where W_{core} is the weight of core microparticles (mg), L is the target coating level (%), and P is the plasticizer-to-polymer ratio (0.10). [15] The calculated solids were dissolved in the organic solvent mixture to attain a standardized working solution (e.g., 1.1% w/v for a 10% coating level). The coating dispersion was applied to the microparticles using a fluidized bed coater / spray-coating assembly under controlled airflow and drying temperatures. The coated microparticles were subsequently cured to ensure complete solvent evaporation. [16]

Table: 1. Coating solution composition example.

Component	Quantity	Calculation	Purpose
Microparticles (batch)	1000 mg	Given	Substrate for coating
Coating level required	10% w/w	Design variable	Target weight gain
Eudragit S100	100 mg	1000 × 10/100	Film-forming polymer
PEG 400	10 mg	100 × 10/100	Plasticizer
Total solids	110 mg	100 + 10	-
Solvent mixture (IPA:Acetone 1:1)	10 mL	5 mL + 5 mL	Volatile solvent
Final concentration	11 mg/mL	110/10	1.1% w/v

Table: 2. Critical process parameters for pan coating.

Process Parameter	Specification	Significance
Core microparticle batch size	10 g	Working batch size
Pan rotation speed	20-25 rpm	Ensures uniform coating
Inlet air temperature	35-40°C	Provides drying without enzyme damage
Maximum bed temperature	<45°C	Critical limit to preserve enzyme activity
Atomizing pressure	1.5-2.0 bar	Controls droplet size
Spray rate	2-3 mL/min	Balances application and drying
Spray gun distance from bed	15-20 cm	Optimal for uniform distribution

Enteric film application was conducted using a laboratory-scale conventional coating pan. Briefly, 10.0 g of dried core microparticles was charged into the pan rotated at 20–25 rpm to maintain uniform bed tumbling. The coating solution was atomized onto the cascading bed

using a pneumatic spray assembly (1.5–2.0 bar atomization air pressure; 2.0–3.0 mL/min delivery rate). [17] To prevent heat-induced denaturation of the entrapped enzymes, inlet air heating was strictly regulated (35–40°C), and the product bed temperature was continuously monitored via an infrared thermometer to ensure it did not exceed 45°C. [18] The process followed an intermittent spray-drying regimen (2 min active atomization followed by a 5 min post-spray drying interval) to prevent over wetting and droplet coalescence until the target theoretical weight gain was attained. [19] Upon completion of the spraying phase, the tumbling bed was dried *in situ* for 15 min without atomization to avert particle agglomeration. The coated microparticles were subsequently transferred to a vacuum desiccator at ambient temperature (25 ± 2°C) for 24 h to eliminate residual volatile solvents. To facilitate polymer chain coalescence, plasticizer redistribution, and complete film maturation, the microparticles were cured at 40°C for 24 h in a precision hot-air oven. [20-21]

Fig.1. Formulation of microparticles.

3. Characterization of optimized formulation

Formulations were dispersed uniformly on a clean glass slide, secured with a coverslip, and visualized under an optical microscope (400× total magnification). Photomicrographs were acquired across multiple representative fields of view using an attached digital imaging system. [22] Morphometric evaluation was conducted using ImageJ software (National Institutes of Health, Bethesda, MD, USA). Feret's diameters of a minimum of 100 randomly selected discrete particles were determined to compute the mean particle diameter, standard deviation ($\pm \text{SD}$), and percentage coefficient of variation ($\% \text {CV} $). [23]

Particle size analysis

Ensemble volume-weighted size distributions were quantified via laser diffraction (Mastersizer series, Malvern Instruments, Malvern, UK) based on Mie scattering theory. Briefly, approximately 100 mg of microparticles was dispersed in non-solubilizing liquid paraffin. The resulting dispersion was gently sonicated (2 min, low energy) to disaggregate loose clusters without fracturing individual matrices. [24]

Fig.2. Statistical diagnostic plots and Pareto chart generated by Design-Expert software for the particle size (µm) response. The figure includes the Half-Normal Plot, Normal Plot, Pareto Chart of Standardized Effects, and Numerical Effect Summary, illustrating the significance and contribution of formulation variables—Sodium Alginate (A), Calcium Chloride (B), Eudragit S-100 (C), and Stirring Rate (D)—and their interactions on particle size. The Shapiro–Wilk test (W = 0.990, p = 0.999) confirms that the residuals follow a normal distribution, indicating an adequate model fit.

Fig.3. Contour plot showing the effect of Sodium Alginate concentration (A, mg) and Calcium Chloride concentration (B, % w/v) on particle size (µm). The response surface was generated using Design-Expert software while Eudragit S-100 concentration (C = 10) and stirring rate (D = 400 rpm) were kept constant. The contour indicates the predicted particle size distribution across the experimental design space, with the red point representing the design point.

Fig.4. The Interaction plot illustrating the combined effect of Sodium Alginate concentration (A, mg) and Calcium Chloride concentration (B, mg/mL) on the particle size (µm) of microparticles. The graph was generated using Design-Expert software while Eudragit S-100 concentration (C = 10) and stirring rate (D = 400 rpm) were maintained at constant levels. The plot demonstrates the interaction between sodium alginate and calcium chloride on the particle size response.

The surface charge of the engineered microparticles reflects the ionization profile of functional matrix groups and dictates physical colloidal stability via electrostatic repulsion. Formulations exhibited net negative zeta potential values distributed between -20 mV and -40 mV, attributable to deprotonated carboxylate moieties ($-\text{COO}^-$) within the cross-linked sodium alginate backbone and terminal methacrylate groups of Eudragit® S100 at neutral pH. Generally, an absolute electrokinetic threshold $\vert\zeta\vert > 30\text{ mV}$ confers robust physical stability against coalescence via interparticle electrostatic repulsions, whereas potentials between 20 and 30 mV denote moderate stability. The measured surface electronegativity ($<-25\text{ mV}$) confirms sufficient electrostatic stabilization of the reconstituted carrier system in physiological fluids prior to mucosal uptake. [25-26]

Fig.5. The contour plot showing the effect of Sodium Alginate concentration (A, mg) and Calcium Chloride concentration (B, mg/mL) on the zeta potential (mV) of enzyme-loaded microparticles. The response surface was generated using Design-Expert software while Eudragit S-100 concentration (C = 10) and stirring rate (D = 400 rpm) were maintained at constant levels. The contour lines represent the predicted zeta potential values across the experimental design space, while the red point indicates the experimental design point.

Fig.6. The main effects plots showing the influence of Sodium Alginate concentration (A, mg), Calcium Chloride concentration (B, mg/mL), Eudragit S-100 concentration (C, % w/w), and Stirring Rate (D, rpm) on the zeta potential (mV) of enzyme-loaded microparticles. The plots were generated using Design-Expert software and illustrate the individual effect of each formulation variable while the remaining factors were maintained at constant levels. Error bars represent the confidence intervals of the predicted response.

Differential scanning calorimetry

Thermal characteristics, physical state transitions, and component compatibility were evaluated using a differential scanning calorimeter (e.g., DSC Q20 / DSC 25, TA Instruments, New Castle, DE, USA). Accurately weighed samples (3–5 mg) of individual pure enzymes (bromelain, papain, serratiopeptidase), individual excipients (sodium alginate, Eudragit® S100), an unprocessed physical mixture, and the optimized enteric-

coated microparticles were hermetically crimped into standard aluminum pans. An empty sealed pan served as the reference. Thermograms were acquired over a dynamic temperature range of 25°C to 300°C at a linear heating ramp of 10°C/min under an ultra-pure nitrogen purge gas (flow rate: 50 mL/min) to maintain an inert atmosphere. [27-28]

Fig.7. The Differential Scanning Calorimetry (DSC) thermogram of the microparticles, recorded over a temperature range of 25–350 °C. The thermogram exhibits a prominent endothermic peak at approximately 55.45 °C, followed by a thermal transition near 66.44 °C, indicating the characteristic thermal behavior of the microparticle.

Fig.8. Differential Scanning Calorimetry (DSC) thermograms of sodium alginate (SD1), calcium chloride (SD2), Eudragit S-100, and drug is physical mixture (SD1). The thermograms were recorded over a temperature range of approximately 25–350 °C, showing the characteristic thermal transitions and thermal stability profiles of the individual components and the physical mixture. Differences in the endothermic and exothermic events indicate the thermal behavior of each material and suggest the absence of significant interactions in the physical mixture.

X-ray diffraction analysis

Powder X-ray diffraction was employed to monitor phase transitions, identify lattice reflections, and evaluate the physical dispersion state of the components within the microparticle architecture (Figure X). Pristine calcium chloride ($CaCl_2$) exhibited an intensely sharp diffraction reflection at $2\theta = 29.39^\circ$, alongside high-angle reflections characteristic of a periodic crystal lattice with long-range molecular order. Conversely, the diffractogram of pristine sodium alginate displayed broad halos superimposed with weak reflections at $2\theta \approx 13.65^\circ, 21.50^\circ, 30.44^\circ, $ and 34.52°, denoting localized semi-ordered chain alignment embedded within an intrinsically amorphous macromolecular network governed by random-coil arrangements and extensive intra/intermolecular hydrogen bonding. [29-30] Similarly, Eudragit® S100 yielded diffuse amorphous envelopes centered around $2\theta \approx 7.97^\circ, 20.71^\circ, $ and 31.81°, confirming a disordered polymeric state suitable for continuous enteric film formation. In the diffractogram of the optimized enteric-coated microparticles, the characteristic sharp crystalline reflections of $CaCl_2$ and any distinct drug peaks were entirely attenuated or absent, giving rise to a broad, diffuse halo pattern. [31] The loss of Bragg reflections indicates significant disruption of native crystal packing during the ionotropic gelation and enteric film deposition processes. Cross-linking between the divalent Ca^{2+} ions and the carboxylate groups of alginate, combined with the continuous Eudragit® S100 envelope, induced extensive matrix amorphization. This transition to an amorphous solid dispersion reflects molecular-level entrapment of the enzyme payload; a state associated with elevated entrapment efficiency, matrix homogeneity, and sustained release kinetics. [32-33]

Fig.9. XRD image of $CaCl_2$

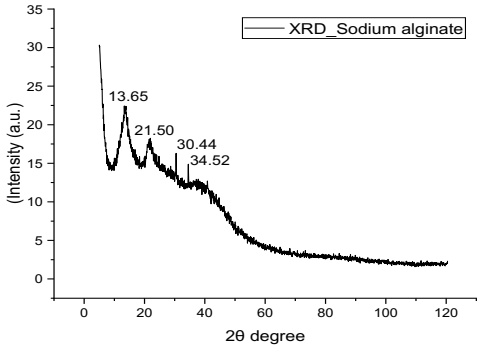


Fig.10. XRD image of sodium alginate.

Fig.11. Eudragit S-100.

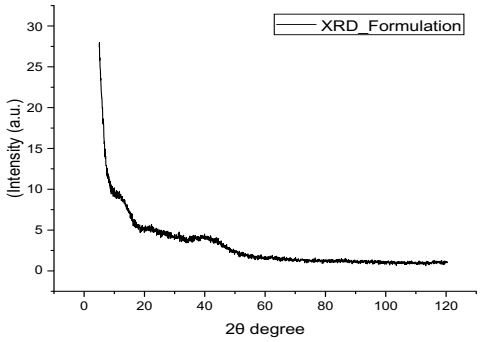


Fig.12. XRD image of formulation.

Scanning electron microscopy

The surface topography, geometric sphericity, and coating integrity of the core and enteric-coated microparticles were examined using a field-emission scanning electron microscope (FE-SEM; e.g., JSM-IT800, JEOL, Tokyo, Japan / Zeiss EVO series). Dried microparticles were dispersed as a non-overlapping monolayer onto aluminum specimen stubs pre-fitted with electrically conductive double-sided carbon adhesive tape. [34] To mitigate surface charging artifacts under the primary electron beam, the mounted specimens were sputter-coated with an ultrathin conductive gold/palladium ($Au\text{–}Pd$) film ($\approx 10\text{–}20\text{ nm}$ thickness) under an inert argon plasma atmosphere for 90–120 s using a high-resolution sputter coater. The stubs were introduced into the specimen analysis chamber and evacuated to a high-vacuum threshold ($10^{-4}\text{ to } 10^{-6}\text{ Torr}$). Micrographs were acquired in secondary electron (SE) imaging mode at an accelerating voltage of 10–20 kV across various working distances and magnifications (50× to 5000×) to evaluate external surface smoothness, shell continuity, and absence of micro-fissuring or agglomeration. [35]

Table: 3. SEM imaging protocol and observations.

Magnification	Size (µm)	Primary Observation	Information Obtained

100-500×	50 µm	Morphology	Shape, size, aggregation
500-1000×	10 µm	Overall particle overview	Size distribution, separation
1000-2000×	10 µm	Surface examination	Coating continuity, surface smoothness
2000-2500×	10 µm	Fine surface details	Pores, cracks, coating defects, texture
2500-5000×	5 µm	Internal structure	Core-shell interface, coating thickness

Fig.13. Scanning electron microscopy.

In-vitro dissolution study: Drug Release in Different pH Iedia (Protease-loaded Microparticles for Colonic Delivery)

In-vitro dissolution testing simulates the gastrointestinal transit of the formulation, evaluating drug release from enteric-coated microparticles under sequential pH conditions that mimic the stomach, small intestine, and colon environments.

Table: 4. Representative drug release data.

Time (h)	pH 1.2 (%)	pH 6.8 (%)	pH 7.4 (%)
0	0	0	0
1	3	8	10
2	6	18	25
4	10	35	50
6	15	50	68
8	18	62	80
12	20	75	90
24	24	88	98

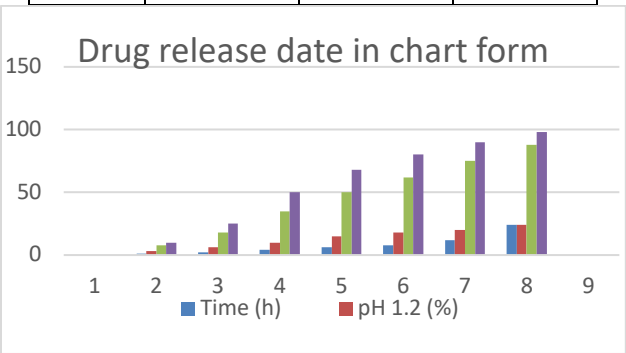


Fig.14. Drug release graph**.**

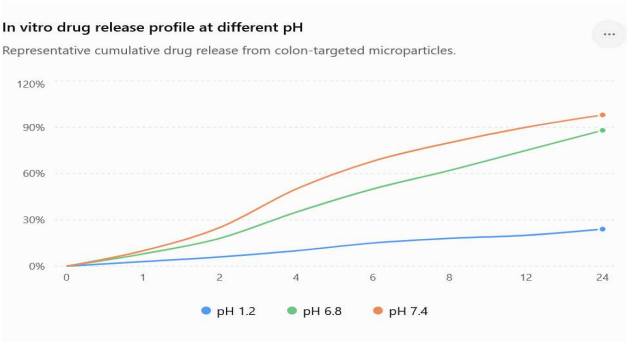


Fig.15. In-vitro drug release profile of enzyme-loaded microparticles in different dissolution media (pH 1.2, pH 6.8, and pH 7.4). The cumulative percentage drug release was evaluated over a 24-hour period. The formulation exhibited minimal drug release at pH 1.2, moderate release at pH 6.8, and maximum release at pH 7.4, demonstrating a pH-dependent and colon-targeted drug release behavior.

Interpretation

pH 1.2 (Simulated Gastric Fluid): Only ~24% drug release was observed over 24 hours, indicating excellent protection of the enzyme loaded microparticle in acidic gastric conditions. pH 6.8 (Simulated Intestinal Fluid): Drug release increased gradually to approximately 88%, suggesting controlled release in the intestinal environment. pH 7.4 (Colonic pH): Nearly complete drug release (~98%) occurred, demonstrating efficient release of the enzyme loaded microparticle in the colon.

4. In-vivo study

The in-vivo evaluation in animal models provides definitive evidence of formulation efficacy by demonstrating colon-specific delivery, therapeutic anti-inflammatory effect, and safety profile in a validated experimental model of colitis.

Selection of animal model for colitis

The experiment will employ 6 treatment groups with 6 rats per group total 36 rats. Group I serves as Normal Control receiving no colitis induction and no treatment, establishing baseline normal parameters for all measurements. Group II serves as Disease Control receiving colitis induction followed by vehicle (0.5% carboxymethyl cellulose solution) only, establishing disease severity and natural progression without therapeutic intervention. [36] Group III receives colitis induction followed by standard reference drug sulfasalazine at dose 100 mg/kg body weight orally once daily, serving as positive control demonstrating expected therapeutic response to standard treatment. Groups IV, V, and VI receive colitis induction followed by test formulation (optimized enzyme-loaded enteric microparticles) at three dose levels: low dose 50 mg/kg enzyme, medium dose 100 mg/kg enzyme, and high dose 200 mg/kg enzyme respectively, allowing dose-response relationship evaluation. [37]

Table: 5. Experimental group design.

Group	No. of groups	Treatment Descriptio	N	Dose	Purpose

		n			
I	Normal group	Normal Control (No colitis, No treatment)	6	-	Establish normal baseline values
II	Acetic acid control group	Disease Control (Colitis + Vehicle)	6	0.5% Acetic acid, 2 mL	Establish disease severity without treatment
III	Standard (Colitis + sulfasalazine -100 mg/kg)	Standard Drug (Colitis + Sulfasalazine)	6	100 mg/kg	Positive control - standard treatment
IV	Low dose Colitis +Microparticle	Test Low Dose (Colitis + Microparticles)	6	50 mg/kg enzyme	Low dose efficacy assessment
V	Medium dose Colitis +Microparticle	Test Medium Dose (Colitis + Microparticles)	6	100 mg/kg enzyme	Optimal dose determination
VI	High dose Colitis +Microparticle	Test High Dose (Colitis + Microparticles)	6	200 mg/kg enzyme	Maximum efficacy and dose-response

Wound/Inflammation Healing/Contraction

(A)



(B)



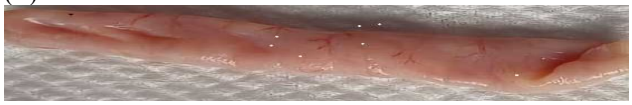
(C)



(D)



(E)



(F)

Fig.16. Effect of microparticle on macroscopic score of (A) controlled group, (B) acetic acid-induced colitis rats, (C) standard drug (sulfasalazine), (D) lower dose of microparticle, (E) medium dose of microparticle, (F) higher dose of microparticle.

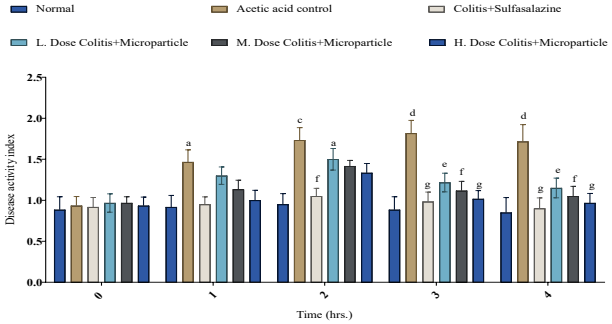


Fig.17. Effect of microparticle treatment on disease activity index (DAI) in acetic acid-induced colitis over time. Disease activity index (DAI) was assessed at 0, 1, 2, 3, and 4 h in normal, acetic acid control, sulfasalazine-treated, and microparticle-treated groups (low, medium, and high doses). Values are presented as mean ± SD. Acetic acid-induced colitis significantly increased the DAI compared with the normal group, whereas treatment with sulfasalazine and microparticles reduced disease severity in a dose-dependent manner. Different superscript letters (a–g) indicate statistically significant differences among groups at the corresponding time point ($p < 0.05$).

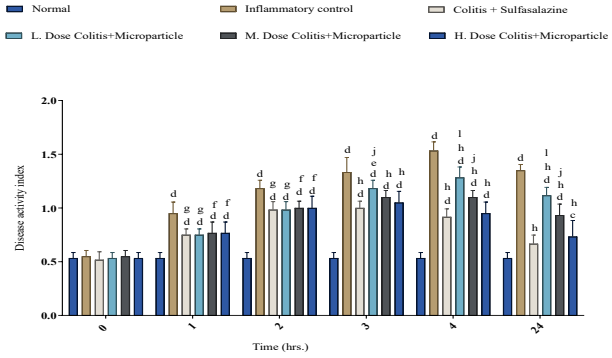


Fig.18. Effect of low-, medium-, and high-dose [papain, bromaline, sarratiopeptidase]-loaded microparticles on the Disease Activity Index (DAI) in an experimental colitis model over 24 h. DAI was recorded at 0, 1, 2, 3, 4, and 24 h for Normal, Inflammatory Control, Colitis + Sulfasalazine, and microparticle-treated groups. Values are expressed as mean ± SD (or SEM). Different superscript letters indicate statistically significant differences among groups at each time point ($p < 0.05$).

5. Evaluation of inflammatory biomarker's

Biochemical evaluation of inflammatory mediators, cytokines, and oxidative stress parameters provides objective quantitative measures of disease severity and therapeutic efficacy at the molecular level.

Table: 6. Observation table of inflammatory biomarkers.

GROUP	IL6	1 BETA	TNF ALPHA

Normal	29.086±5.528	13.633 ±*3.662*	14.70 ±*4.46*
Acetic acid Control	92.531±7.448^{d}	39.773 ±*7.336*^{c}	60.6 ±*14.23*^{b}
Colitis+Sulfasalazine	45.883±14.039^{f}	19.60 ±*3.687*^{bj}	26.1 ±*7.33*^{e}
Low dose Colitis+Microparticle	63.866±11.599^{ae}	28.516 ±*4.713*^{f}	42.61 ±*4.70*^{ci}
Medium. dose Colitis+Microparticle	53.675 ±*11.465*^{f}	23.316 ±*7.202*^{f}	37.93 ±*5.20*^{bei}
High. dose Colitis+Microparticle	41.066 ±*8.288*^{g}	15.576 ±*4.748*^{f}	22.85 ±*6.33*^{f}

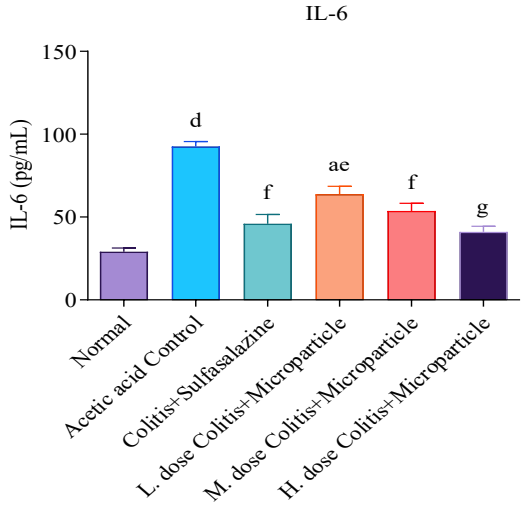


Fig.19. Graph of IL-6

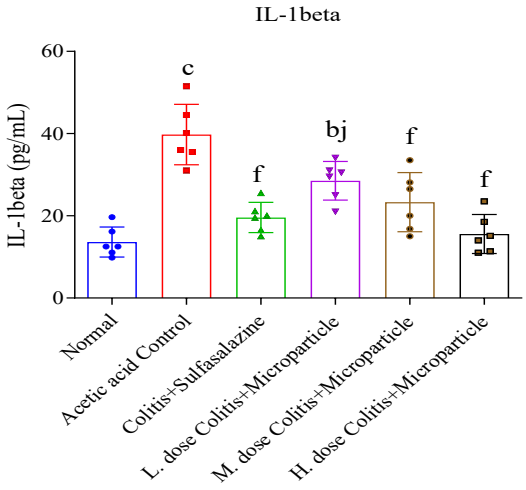


Fig.20. Graph of IL-1beta

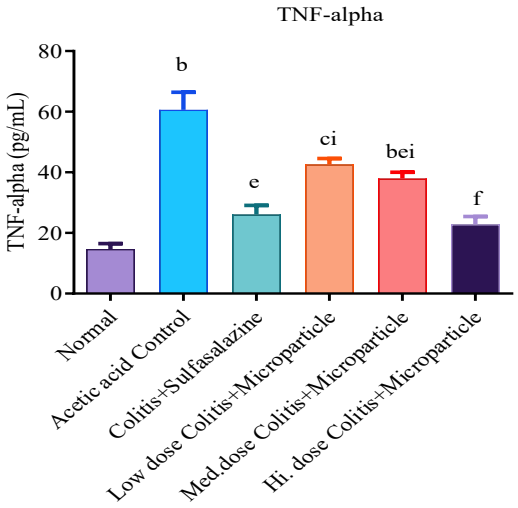


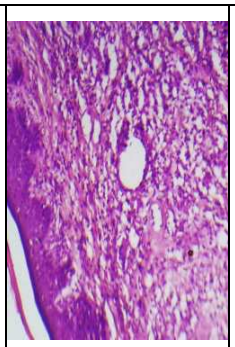
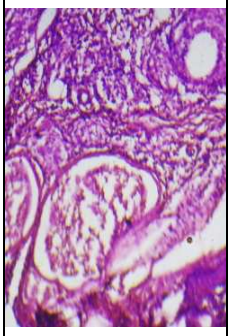
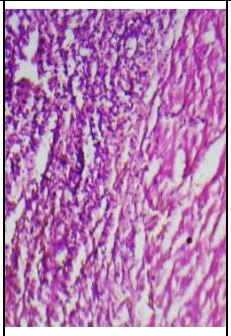
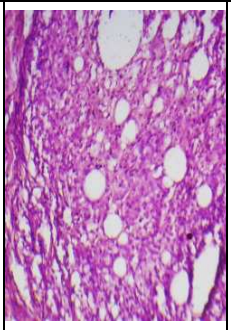
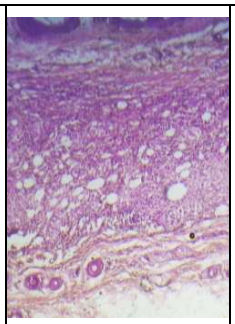
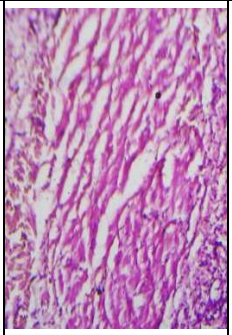
Fig.21. Graph of TNF - alpha

Histological evaluation of colonic mucosa

Histological examination provides definitive microscopic assessment of inflammation severity, mucosal architecture, cellular infiltration, and healing response. The formalin-fixed distal colon segments undergo tissue processing. [23]

Table: 7. Histological evaluation of colonic mucosa.

S. No.	**Group**	**Colonic Mucosa Histology**	**Treated Dose**

1.	Group-I		Normal group
2.	Group-II		Control group
3.	Group-III		Standard (Colitis + sulfasalazine - 100 mg/kg)
4.	GROUP-IV		Low dose Colitis + Microparticle (50 mg/kg, per.os.)
5.	Group-V		Medium dose Colitis + Microparticle (100 mg/kg, p.o.)
6.	Group-VI		High dose Colitis + Microparticle (200 mg/kg, p.o.)

6. Results and Discussion

Colon-targeted microparticles containing bromelain, papain, and serratiopeptidase were successfully developed using the ionic gelation technique, with sodium alginate as the primary polymer and colon-specific coating polymers to enhance gastrointestinal protection and site-specific enzyme release. The prepared formulations exhibited satisfactory physical characteristics, while production yield and encapsulation efficiency were evaluated to assess formulation performance. The optimized formulation was selected based on particle size, encapsulation efficiency, and in vitro release characteristics, demonstrating the potential of this polymeric delivery system for colon-targeted enzyme delivery. The optimized microparticles exhibited a zeta potential ranging from −28 to −35 mV, indicating a substantial negative surface charge attributed to the ionized carboxyl groups of sodium alginate, which may contribute to improved dispersion stability. Differential scanning calorimetry (DSC) revealed broader and less intense thermal peaks in the optimized formulation compared with the pure enzymes, suggesting changes in their thermal behavior following incorporation into the polymeric matrix.

These findings support successful formulation development; however, further stability and enzymatic activity studies are required to confirm long-term stability and preservation of enzyme functionality. X-ray diffraction (XRD) analysis revealed reduced peak intensity and broader diffraction patterns in the optimized microparticles compared with the pure enzymes, suggesting reduced apparent crystallinity or dispersion of the enzymes within the polymeric matrix. Scanning electron microscopy (SEM) demonstrated predominantly

spherical microparticles with relatively smooth surfaces and minimal aggregation or visible defects, indicating effective particle formation through ionic gelation. These findings support successful incorporation of the proteolytic enzymes into the polymeric matrix; however, further enzymatic activity studies are required to confirm protection against gastrointestinal degradation. In vitro dissolution studies demonstrated pH-dependent enzyme release, with less than 10% release in simulated gastric fluid (pH 1.2), approximately 20–35% release in intestinal fluid (pH 6.8) after 5 hours, and over 85–90% cumulative release under simulated colonic conditions (pH 7.4) within 24 hours. [38]

These findings indicate the potential of the developed microparticles for pH-responsive colon-targeted delivery. In vivo evaluation further demonstrated reduced disease severity, improved colonic tissue architecture, and favorable changes in inflammatory cytokines and oxidative stress markers compared with untreated controls, suggesting potential therapeutic benefits of the formulation. The developed bromelain-, papain-, and serratiopeptidase-loaded microparticles demonstrated promising physicochemical characteristics and pH-dependent release behavior, with limited release under simulated gastric conditions and enhanced release in simulated colonic fluid. The reported in vivo findings indicated improvements in disease severity, inflammatory and oxidative stress markers, and colonic histopathology. Collectively, these results highlight the potential of ionic gelation-based microparticles for colon-targeted protease delivery. Further investigations into enzymatic activity, formulation stability, gastrointestinal localization, and statistically validated therapeutic outcomes are necessary to establish their suitability for pharmaceutical applications.

The present study successfully developed protease-loaded colon-targeted microparticles using the ionic gelation technique. The optimized formulation exhibited favorable physicochemical properties, spherical morphology, and pH-dependent release characteristics. Thermal and crystallographic analyses revealed changes in the physicochemical characteristics of the enzyme–polymer system following encapsulation. The formulation demonstrated limited enzyme release under simulated gastric conditions and enhanced release under simulated colonic conditions, indicating its potential for site-specific delivery. Overall, the developed microparticles represent a promising platform for colon-targeted protease delivery in inflammatory bowel disease, warranting further validation of enzyme activity, gastrointestinal stability, and in vivo therapeutic efficacy. [39]

7. Conclusion

The present study successfully developed and characterized colon-targeted microparticles containing bromelain, papain, and serratiopeptidase using the ionic gelation technique. The optimized formulation demonstrated favorable physicochemical properties, including an appropriate particle size distribution, negative zeta potential, satisfactory encapsulation characteristics, and desirable surface morphology. Differential scanning calorimetry (DSC) and X-ray diffraction (XRD) analyses revealed changes in the thermal and solid-state characteristics of the enzyme–polymer matrix following encapsulation, while scanning electron microscopy (SEM) confirmed the formation of predominantly spherical microparticles with relatively smooth surfaces. In vitro dissolution studies demonstrated limited enzyme release under simulated gastric conditions, followed by enhanced release in simulated colonic fluid, supporting the potential of the formulation for pH-responsive colon-targeted delivery. This delivery approach may help protect the encapsulated enzymes during gastrointestinal transit and facilitate localized release at the intended site. Overall, the developed microparticles represent a promising platform for oral protease delivery in inflammatory bowel disease. Further investigations into enzymatic activity, formulation stability, in vivo efficacy, and long-term safety are required to establish their therapeutic potential and clinical applicability.

References

1. Wu, C., Bi, C., Kim, G. S., et al. (2025). Oral colon-targeted responsive chitosan/pectin-based nanoparticles propels the application of tofacitinib in colitis therapy. Scientific Reports, 15, 1569.

2. Xu, Y., Zheng, X., Wang, Y., et al. (2025). Colon-targeted mucoadhesive PLGA microspheres loaded with Ramulus Mori alkaloids for enhanced water-soluble drug delivery in ulcerative colitis treatment. Molecules, 30(9), 1878.

3. Wei, X., Chen, L., Liu, Y., et al. (2025). Classification of nanomaterial drug delivery systems for inflammatory bowel disease. Drug Design, Development and Therapy, 19, 621–648.

4. Li, H., Wang, L., Sun, X., et al. (2024). Combining gut microbiota modulation and enzymatic-triggered colonic delivery by prebiotic nanoparticles improves mouse colitis therapy. Biomaterials Research, 28, 0062.

5. Gautam, P., Akhter, M., & Anand, A. (2024). A novel mesalamine loaded hybrid nanoparticle-in-microparticle for colon targeting: In-vitro and in-vivo investigations. Journal of Pharmaceutical Innovation, 19, 75.

6. Zhu, Y., Chen, X., Wang, H., et al. (2024). Nanoparticle-based drug delivery systems for inflammatory bowel disease treatment. Drug Design, Development and Therapy, 18, 2921–2949.

7. Gazzi, A., Pomelli, C., Bianco, A., et al. (2024). Bioinspired and bioderived nanomedicine for inflammatory bowel disease. WIREs Nanomedicine and Nanobiotechnology, 16(4), e1986.

8. Wang, P., Liu, Q., Chen, R., et al. (2024). The proteolytic activity in inflammatory bowel disease: Insight from gut microbiota. Microbial Pathogenesis, 190, 106617.

9. Hansson, G., Sandoval-Guzman, T., & Bhatt, D. (2024). Proteolytic bacteria expansion during colitis amplifies inflammation through cleavage of the external domain of PAR2. Gut Microbes, 16(1), 2387857.

10. Chen, Z. J., Wang, T., Zhao, H., et al. (2024). Spatio-temporally controlled all-in-one hydrogel microspheres for ulcerative colitis treatment based on cocktail strategy. Chemical Engineering Journal, 498, 155021.
11. Sarkar, A., Banerjee, S., Das, P., et al. (2024). Inulin-based colon-targeted drug delivery systems: Advancing site-specific therapeutics. Discover Materials, 4, 32.
12. Lopes, S. A., Roque-Borda, C. A., Duarte, J. L., Di Filippo, L. D., Cardoso, V. M. B., Pavan, F. R., Chorilli, M., & Meneguin, A. B. (2023). Delivery strategies of probiotics from nano- and microparticles: Trends in the treatment of inflammatory bowel disease—An overview. Pharmaceutics, 15(11), 2600.
13. Zhang, Y., Wang, L., & Wang, Z. D. (2023). Surface-anchored microbial enzyme-responsive solid lipid nanoparticles enabling colonic budesonide release for ulcerative colitis treatment. Journal of Nanobiotechnology, 21, 145.
14. Caminero, A., Guzman, M., Libertucci, J., & Lomax, A. E. (2023). The emerging roles of bacterial proteases in intestinal diseases. Gut Microbes, 15(1), 2181922.
15. Carvalho, S. G., dos Santos, A. M., Polli Silvestre, A. L., Tavares, A. G., Chorilli, M., & Gremião, M. P. D. (2023). Multifunctional systems based on nano-in-microparticles as strategies for drug delivery: Advances, challenges, and future perspectives. Expert Opinion on Drug Delivery, 20(9), 1231–1249.
16. Guo, J., Caminero, A., Turpin, W., Bermudez-Brito, M., Santiago, A., Libertucci, J., & Constante, M. (2023). Crohn's disease proteolytic microbiota enhances inflammation through PAR2 pathway in gnotobiotic mice. Gut Microbes, 15(1), 2205425.
17. Zhang, Y., Ma, R., You, C., Leng, X., Wang, D., & Deng, S. (2023). Hyaluronic acid modified oral drug delivery system with mucoadhesiveness and macrophage-targeting for colitis treatment. Carbohydrate Polymers, 313, 120884.
18. Sanz-Moros, A., Larrañeta, E., & Donnelly, R. F. (2023). Rationalized design to explore the full potential of PLGA microspheres as drug delivery systems. Drug Delivery, 30(1), 2219864.
19. Tie, H., Wang, Y., Shang, Y., Li, M., Wei, X., & Wang, Z. (2023). Fabrication of pH-dependent solid dispersion for oral colon-targeted delivery of notoginsenoside R1 and its protective effects on ulcerative colitis mice. Heliyon, 9, e20280.
20. Abhay Padalkar N, Sadhana Shahi R, Mahesh Thube W. Micro particles: an approach for betterment of drug delivery system, International Journal of Pharmaceutical Research & Development, 2012.
21. Pavan Kumar B, Sarath Chandran I, Bhavya B, Sindhuri M. Micro particulates drug delivery system: a review, Indian journal of Pharmaceutical Science and Research. 2011;3:19-32.
22. Edith Mathiowitz, Mark Kreitz R, Lisa Brannon-Peppas. Microencapsulation. Outline. 2008;5(2):495-496.
23. Nymkamp G, Carstensen V, Mullar BW. Jet milling-a new technique for Micro particles preparations, International Journal of Pharmaceutics, 2002, 79-86.
24. Gattani YS. Floating Multiparticulate Drug Delivery Systems: An Overview International Journal of Pharmacy and Biosciences. 2010;6(2):35-40.
25. Jain NK. Controlled and Novel Drug Delivery, 4th Edition, New Delhi: CBS Publishers and Distributers, 2002, 236-237.
26. James Swar Brick, James Boylan E, Mercel Dekkar. Microencapsulation technology and applications. Encyclopedia of pharmaceutical Technology. 1988;10:245-286.
27. Kinam Park, Yoon Yeo. Microencapsulation technology encyclopedia of pharmaceutical technology GEPT. 2002;6(2):67-85.
28. Langer R, Folk Man J. Polymers for the Sustained Release of Proteins and Other Macromolecules, Nature. 1976;263:797-800.
29. Dixit MP. Preparation and characterization of microparticles of piroxicam by spray drying and spray chilling methods. [Pub Med] Central (PMC), 2019.
30. Mehnertw Maderk. Solid Lipid Nanoparticles: Production, Characterization and Applications. Adv. Drug Delivery. Rev. 2001;47:165-196. Excellent Review of SLNs.
31. Moore J. The Drug Delivery Outlook to 2005. Business Insights Ltd., 1999.
32. Satheesh Madhav NV, Shivani Kala. Review of micro particles drug delivery system, International Journal of Pharm. Tech Research. 2011;3:1242-1254.
33. Passerine, Perissuttib. Albertinibetal: Controlled Release of Verapamil Hydrochloride from Waxy Micro particles Prepared By Spray Congealing. J. Control. Release. 2003;88(2):263-27.
34. Plamen K, Bissera P, Margarita K. Preparation techniques of micro particles for drug delivery, 2019.
35. Putney SD, Burke PA. Improving Protein Therapeutics with Sustained Release Formulations, Nature Biotechnology. 1998;16:153-157.
36. Rama Dubey, Shamc TC, Bhaskar Rao KV. Microencapsulation technology and applications.Defence Science Journal. 2009;59(1):82-83.
37. Thies C. Microencapsulation. In: Encyclopedia of Polymer and Engineering, J. I. Kroschwitz, H. F. Mark, N. M., 1987.
38. Veronica Lassalle, Maria Lujan Ferreira. PLA Nano- and micro particles for drug delivery: an overview of method of preparations, Macromolecular Bioscience, 2007, 767- 783.
39. Vyas SP, Khar RK. Targeted and Controlled Drug Delivery Novel Carrier System, 1st Edition, New Delhi: Cbs Publishers and Distributers, 2002, 419-42.